IEEE Photonics Journal
An IEEE Photonics Society Publication

Controllable Formation of Si Nanostructures Based on Quasi-Plasmonic Planar Nanostructures Formed by Annular-Shaped Femtosecond Laser Pulse

Volume 11, Number 4, August 2019

Weina Han
Dongfang Li
Furong Liu
Yanping Yuan
Xiaowei Li

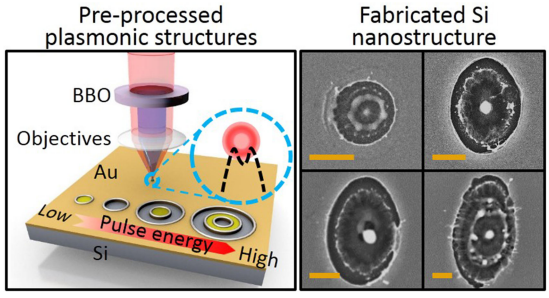

DOI: 10.1109/JPHOT.2019.2930801

IEEE photonics SOCIETY
IEEE

Controllable Formation of Si Nanostructures Based on Quasi-Plasmonic Planar Nanostructures Formed by Annular-Shaped Femtosecond Laser Pulse

Weina Han,[1,2] **Dongfang Li**,[2] **Furong Liu**,[2] **Yanping Yuan**,[2] **and Xiaowei Li**[1]

[1]Laser Micro/Nano Fabrication Laboratory, School of Mechanical Engineering, Beijing Institute of Technology, Beijing 100081, China
[2]Beijing Engineering Research Center of Applied Laser Technology, Institute of Laser Engineering, Beijing University of Technology, Beijing 100124, China

DOI:10.1109/JPHOT.2019.2930801

Manuscript received April 30, 2019; revised July 9, 2019; accepted July 21, 2019. Date of publication July 23, 2019; date of current version August 7, 2019. This work was supported in part by the Beijing Natural Science Foundation under Grant 3194045, in part by the National Key R&D Program of China under Grant 2018YFB1107401, in part by the Research Foundation from Ministry of Education of China under Grant 6141A02033123, in part by the National Natural Science Foundation of China (NSFC) under Grant 51805014 and Grant 51705328, in part by the Beijing Municipal Education Commission Foundation under Grant KM201910005003 and Grant KM201910005004. Corresponding author: Yanping Yuan (e-mail: ypyuan@bjut.edu.cn).

This paper has supplementary downloadable material available at http://ieeexplore.ieee.org, provided by the authors.

Abstract: We demonstrate the feasibility to control the confined electromagnetic field by surface plasmon poloritons (SPPs) excitation and scattering modulation based on the pre-processed Au nanostructures under the irradiation of single-shot femtosecond (fs) laser pulse, and then to control the surface tension-induced molten Si transport due to the directed lateral temperature profile, thus resulting in the formation of Si nanostructures. Annular-shaped fs laser pulse is employed based on nonlinear optical effect of frequency-doubling process to imprint Au planar nanostructures with various morphologies. Because surface plasmon polaritons can be easily excited and controlled on planar nanostructures of noble metals, the localized electromagnetic field can be effectively modulated by controlling the metallic nanostructures. Thus, the quasi-plasmonic Au nanostructures act as precursors for controlling the subsequent electromagnetic field by fs laser irradiation. Upon irradiation of pre-processed Au nanostructures, confined electromagnetic field induces a specific surface tension profile, causing directional transport of molten Si. After solidification, Si nanostructures of controllable morphologies can be fabricated. Simulation results are in agreement with the theoretical mechanism. Moreover, further optimized modulation of nanodome can be achieved by controlling the focus spot control combined with the polarization state control. This paper provides an effective method for enabling a scalable formation of Si nanostructures.

Index Terms: Annular-shaped femtosecond laser, surface plasmon polaritons, planar metallic nanostructure, Si nanostructures.

1. Introduction

Ordered micro/nano-patterning of Si with controllable morphologies has attracted considerable interests because of its promising applications in photonics [1], [2], microelectronics [3], microfluidics [4[, [5], solar cells [6], surface enhanced Raman scattering (SERS) [7], water-repellent surfaces [5], [8], and sensors [9]. The crucial parameters affecting the properties of a fabricated micro-/nanopatterned Si surface are the phase (crystal or amorphous), size, geometrical morphology, and arrangement of single micro-/nanostructures [2], [10], [11]. Thus, it is crucial to precisely control the morphology of Si micro- and nanostructures. Compared with conventional surface micro- and nanopatterning technologies, a femtosecond (fs) laser has proved to be a promising tool for micro- and nanopattering on bulk materials surfaces owing to its ultrashort irradiation period and ultrahigh-intensity properties. These unique properties in some cases fundamentally change the laser-material interaction mechanisms, thus leading to ultrahigh quality and precision processing [12], [13].

Up to now, fs laser pulses has been applied in the surface micro/nanostructures fabrication with various morphologies on bulk Si through laser direct writing approach [14]–[18]. However, the precise fabrication and control of single nanostructure unit is still of big challenge. Researches demonstrate that upon irradiation with a focused laser pulses, the directional transport of the melted materials gives the possibility to control the morphology of fabricated micro-/nanostructures [19]–[23]. This effect is based on the hydrodynamic control of the melted materials caused by the specific temperature gradient induced by the deposited electromagnetic field. Thus, it is vital to steer the precise control of electromagnetic field, which determine the final processing micro/nanostructures.

The emerging field of plasmonics based on the excitation of surface plasmon poloritons (SPPs) allows manipulation of electromagnetic field at subwavelength scales due to its unique properties of SPPs [24], [25]. In particular, the realization of steering SPPs on thin films and planar noble metallic nanostructures gives possibilities in manipulating the electromagnetic fields with high precision [24]–[26]. Usually, metallic nanostructures exhibit desirable responses to electromagnetic fields, which based on the geometry morphology, material, and arrangement of the nanostructures [26]–[28]. Thus, we attempt to control the confined electromagnetic field by the SPPs excitation and scattering control through pre-processed plasmonic nanostructures, and control the directional transport of molten Si by the surface tension because of the lateral temperature profile. Consequently, Si nanostructures with controllable morphologies can be formed.

In this study, SPPs induced by the pre-processed Au nanostructures on a Si surface are used to manipulate the electromagnetic field by fs laser irradiation. The fabrication of Si nanostructures is controlled through the modulated transport of the melting materials based on the specific electromagnetic field control. Concentric annular nanostructures are imprinted on Au thin films by irradiation with annular-shaped single-shot fs laser pulse through conducting the frequency doubling process. The obtained pre-processed concentric annular Au nanostructures exhibit a quasi-plasmonic effect, which enables modulation of the electromagnetic field on the Si surface. The electromagnetic field control and enhancement effect enables the formation of Si nanostructures by single-shot fs laser pulse irradiation. Si nanostructures with various morphologies such as nanodome, nanohole, and nanocrown are easily fabricated by controlling the morphology of the pre-processed Au nanostructure. Moreover, when spot size control is combined with polarization state control, an optimized morphology modulation of the Si nanodome is realized. The micro-/nanostructures can be set to the pre-defined state with high selectivity by using various types of metallic nanostructures.

2. Fabrication process

The controllable Si nanostructures fabrication process is schematically presented in Fig. 1(a), similar with that in our previous study [14]. The fs laser source is a Ti:sapphire laser regenerative amplifier system that provide a fundamental Gaussian mode with a central wavelength of 800 nm (λ_1), pulse duration of 50 fs, and repetition rate of 1 kHz. The dual-color waveform is realized by frequency doubled in a Type I beta barium borate (β-BBO) crystal in front of the focusing objective

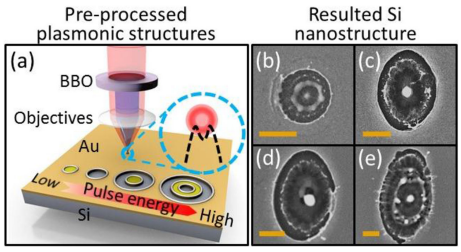

Fig. 1. (a) Illustration of the pre-processed Au nanostructures fabricated by single-shot dual-color fs laser pulse. (b)–(e) SEM images of the Si nanostructures based on printed Au nanostructures fabricated by a single dual-color fs laser pulse with increased pulse energies: (b) 3 nJ, (c) 8 nJ, (d) 9 nJ, and (e) 40 nJ (scale bar: 2 μm).

to generate 2ω pulses at 400 nm (λ_2). The energy ratio ($E_{2\omega}/E_{\omega}$) is controlled by adjusting the incident angle to a maximum value of approximately 25%. The pulse energy is varied using a variable neutral density filter. A half-wave plate or a quarter-wave plate is used to change the linearly polarization direction of the incident laser pulse (λ_1) or achieve a circular polarized fs laser pulse. The highly polished Si is sputtered with a 30-nm Au thin film. Initially, Au nanostructures with various morphologies are imprinted using a single dual-color fs laser pulse by controlling the irradiated pulse energy and focused spot. Particularly, in this study, objectives of $4\times$ and $10\times$ are used to change the focused spot size on the sample surface, which reduce the size of the pre-process Au structures to modulate the SPPs field based on quasi-plasmonic focusing effect; while with the large spot size shown in our previous study [14], the SPPs-laser interference effect is used to control the morphology of the ripple structures by single-shot fs laser pulse excitation. Then, the pre-processed Au nanostructures are irradiated by another single-shot dual-color fs laser pulse. By modulating the SPPs-enhanced localized electric field, Si nanostructures with different morphologies can be fabricated (Figs. 1(b)–(e)).

3. Results and Discussion

3.1 Pre-Processed Plasmonic Concentric Annular Micropatch Structure Fabricated Using an Annular-Shaped fs Laser Pulse

The geometrical morphology of the ablated surface structures can imprint the real beam shape of the irradiated laser pulse [19]. According to our previous studies [14], [23], three different surface morphologies can be imprinted on Au thin film by changing the dual-color fs laser pulse energies (see Figs. S1(a)–(h) in Supplementary Material for details). Through hole with one bumped circle, concentric annular structure with two circles, and concentric annular structure with three circles are successively formed by increasing pulse energy from 5 nJ to 55 nJ. The bumped circles are manifested by the detailed AFM measurement. The spatial pulse shaping effect is caused by the frequency doubling process, leading to an annular energy distribution of the fundamental fs laser pulse [14], [23]. The higher conversion efficiency in the central part of the Gaussian-shaped laser beam results in the lower pulse energy of the fundamental fs laser pulse after the frequency doubling by BBO crystal, which leads to an annular intensity distribution. Furthermore, the laser pulse of 400 nm has no fabrication effect in this research, which exhibits that the fabricated surface structures are dominated by the annular-shaped fundamental laser pulse (λ_1).

3.2 Morphology Modulation of the Si Micro-/Nanostructure Based on the Pre-Processed Concentric Annular Nanostructure by Using a Single-Shot fs Laser Pulse

According to the previous researches, subwavelength nano-slits or nano-corrals are common planar nanoscale metallic structures for SPPs modulation [26], [27]. In this study, the imprinted concentric Au nanostructures with bumped are confirmed to be nanometer in scale by using AFM analysis, which can be considered as planar metallic nanostructures. Thus, we can deduce that the Au

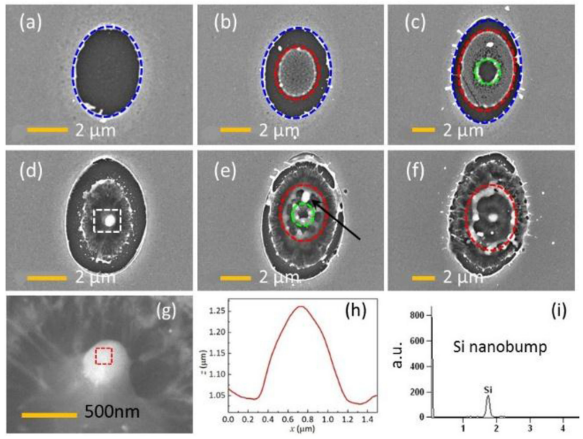

Fig. 2. (a)–(c) SEM images of the Au nanostructures at various pulse energies: (a) 8 nJ, (b) 20 nJ, and (c) 25 nJ. (d)–(f) SEM images of the corresponding Si nanostructures. (g) Magnified SEM image of Si nanostructure shown in (d). (h) AFM profile of Si nanodome shown in (g). (i) EDS detection of Si nanodome.

bumped concentric annular nanostructure enables a quasi-plasmonic effect, which can be used to control the electromagnetic field.

Figures 2(a)–(c) present SEM images of the three specific morphologies of the concentric annular Au nanostructures formed by a single-shot dual-color fs laser pulse. The Au nanostructure is fabricated as a precursor for SPPs excitation and propagation for the subsequent electromagnetic field control. Figures 2(d)–(f) present SEM images of the corresponding fabricated Si structures based on the Au nanostructures by another single-shot dual-color fs laser pulse irradiation, and the pulse energy is fixed. As presented, Si nanostructures at the location of the central Au nanostructures are fabricated with various morphologies. Si nanodome (Figs. 2(d) and 2(g)) with a diameter around 470 nm can be fabricated based on the Au nanostructure with one bumped circle, and it keeps a crystalline state demonstrated by EDS detection (Fig. 2(i)). Nevertheless, the central nanoscale materials are removed from the Si surface based on the Au nanostructures with two bumped circles, leading to the formation of a nanohole with a diameter approximately 650 nm (Fig. 2(e)). In this condition, the removed nanodome displayed in Fig. 2(e) validates an electromagnetic field enhancement on the central part of Au nanostructures. For the third regime with three bumped circles, Si nanodome surrounded by a Si nanoring (Fig. 2(f)) with diameter around 420 nm can be formed. Bumped profile of the nanodome is confirmed by the detailed tilted SEM and AFM detection (Figs. 2(g)–(h)), and the material characterization is confirmed by the energy dispersive (EDS) detection (Fig. 2(i)). To confirm the effect the pre-processed Au nanostructures for the formation of the nanostructures on Si surface, identical experiment is performed on bulk Si surface without the pre-processed Au nanostructures, typical modification area (Fig. S2(a) in the Supplementary Material) and concave microholes (Fig. S2(b), (c) in the Supplementary Material) can be found in this condition. No bumped/sunk nanostructures are found with fundamental fs laser irradiation. Previous studies demonstrate that surface structures following laser irradiation are formed mainly because of the directional surface tension induced by the electromagnetic field transferring the molten material toward specific directions [19]–[23]. Thus, the results of the present study indicate that the pre-processed concentric annular Au nanostructures play an important role in the formation and modulation of bumped or sunken Si nanostructures.

Based on the aforementioned experimental results, we can deduce that the geometrical morphology of Au nanostructures plays an important role in the resulted Si nanostructures morphologies. Specific experiments are performed to validate this effect, as shown in Fig. 3(a)–(c), Au nanostructures with one bumped circle are fabricated at varying energies. The dimension of the Au nanocircles grows as the pulse energy increases. Figures 3(d)–(f) present SEM images of the corresponding fabricated Si nanodomes. The results reveal that the diameter of the Au nanostructure

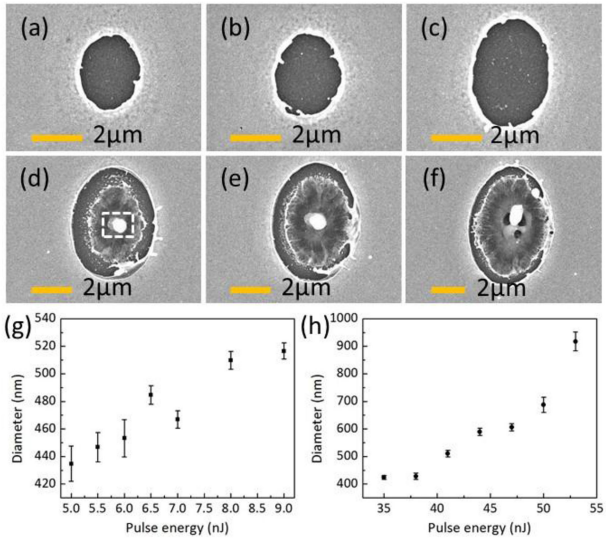

Fig. 3. (a)–(c) Au nanostructures SEM images at different pulse energies: (a) 5 nJ, (b) 7 nJ, and (c) 9 nJ. (d)–(f) Corresponding Si nanostructures based on Au nanostructures shown in (a)–(c). Effect of laser energy on Si nanodome diameter based on Au nanostructure with one bumped circle (g) and three bumped circles (h).

affects the morphology of the Si nanodome. Relatively regular shapes (Figs. 3(d) and 3(e)) are noted based on Au nanocircles with small diameters (Figs. 3(a) and 3(b)). However, Si nanodome is ejected from the bulk Si by exerting an upward-directed momentum [29], thus leaving a hole in the Si substrate. As seen, Fig. 3(c) shows the critical state of this ejection effect. Figures 3(g) and 3(h) present the effect of irradiated pulse energy on the diameter of the formed Si nanodome based on Au nanostructures with one bumped circle and three bumped circles, respectively. For the first regime with one bumped circle, the diameter of the Si nanodome is in the range of 434–516 nm at laser energy between 5 and 9 nJ (Fig. 3(g)). For Au nanostructure with three bumped circles, larger nanodome can also be produced (Fig. 3(h)). The diameter of the Si nanodome ranges from 424 nm to 917 nm at a laser energy between 35 nJ and 53 nJ. We attribute the increased diameter of the nanodome at higher pulse energies to the increased volume of molten materials.

3.3 Numerical Simulation and Theoretical Analysis Based on the Pre-Processed Plasmonic Surface Metallic Nanostructures

The profile of the pre-processed Au nanostructures resembles that of quasi-plasmonic corral structures so that SPPs scattering can be controlled within the Au nanocorral. Specific surface tension induced by the modulated electromagnetic field distribution is proposed to explain the fabrication and modulation of Si nanostructures, which drive the directional mass transfer of the molten Si. To comprehensively explain the physical mechanism of the quasi-plasmonic effect, we use numerical simulation to calculate the electric field distribution on a pre-designed concentric annular ring Au nanostructure with different morphologies. Based on the experimental measured profile of the concentric annular ring nanostructure, the geometry of the circular nanocorral for the three regimes can be described by six parameters, d_1, d_2, d_3, h_1, h_2, and d, as present in Figs. 4(a)–(c). The Au dielectric function is obtained from the experimental data of Johnson and Christy [30]. The complex refractive index of Si would be dramatically modified due to the high density of the excited free electrons [31]. In this study, the pulse energies we use are near the ablation threshold of Si for a single shot. The real part of the refractive index remains nearly unchanged; however, a significant increase in κ is expected. Thus, the complex refractive index of Si is chosen to be $n = 3.4 + i0.5$ in the numerical simulations [31]. Based on the experimental observations, d_1, h_1, and d were set to

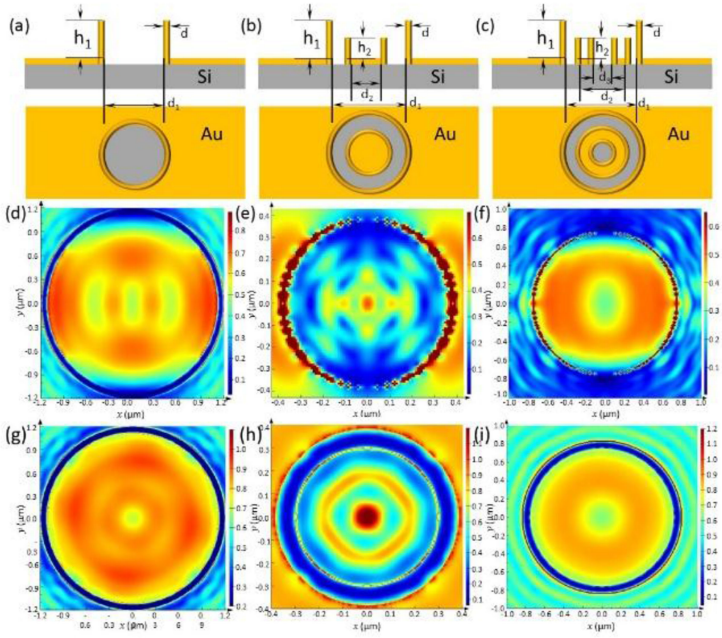

Fig. 4. (a)–(c) Schematic showing the geometry of the pre-processed Au nanostructures with three different morphologies. (d)–(f) The corresponding calculated electric field distributions along *x*-*y* plane with linearly polarization condition. (g)–(i) Calculated *E* distribution under circular polarization condition.

be 2.24 μm, 250 nm, and 80 nm, respectively, in the first regime with one bumped circle. Moreover, for the second regime with two bumped circles, d_1, d_2, h_1, h_2, and d are set to be 2.84 μm, 0.6 μm, 250 nm, 100 nm, and 80 nm, respectively. For the third regime with three bumped circles, d_1, d_2, d_3, h_1, h_2, and d are set to be 5 μm, 4 μm, 1.5 μm, 250 nm, 100 nm and 80 nm, respectively. The electric field (E) distributions of SPPs scattered on the surface of the Si surface in the three different regimes are presented in Figs. 4(d)–(f), respectively. The simulation results demonstrate that the electric field reach a minimum at the center for that with one bumped circle and the third nanostructure with three bumped circles, as presented in Figs. 4(d) and 4(f). In these two regimes, the imposed temperature gradient induces a surface tension gradient that drove the molten silicon fluid from the hot periphery (lower surface tension) to the cold center (higher surface tension). Conversely, the electric field in the second regime with two bumped circles demonstrates a maximum value at the center (Fig. 4(e)). Thus, the material transport is in the opposite direction which results in the nanohole formation.

3.4 Fine Control of the Si Micro-/Nanostructure by Shrinking of the Pre-Processed Plasmonic Surface Metallic Nanostructures

The aforementioned experimental and numerical results indicate that the pre-processed concentric annular Au nanostructures act as precursors for the subsequent SPPs excitation, and the geometric morphology of the pre-processed quasi-plasmonic Au nanostructures is crucial in the modulation of SPPs scattering. Notably, the numerical simulation results show an anisotropic localized electric field distribution. However, the morphology of the fabricated nanodomes show nearly isotropic morphologies. During the bumped Si nanodomes formation, the thermocapillary force would balance the anisotropic effect, driving the molten silicon shrink into a hemispherical morphology (with minimum volume). Meanwhile, the annular intensity distribution of the dual-color fs laser pulse, which induces an isotropic donut distribution may also balance the anisotropic effect. Whereas, according to the experimental results this anisotropic effect does affect the fabricated results, which results

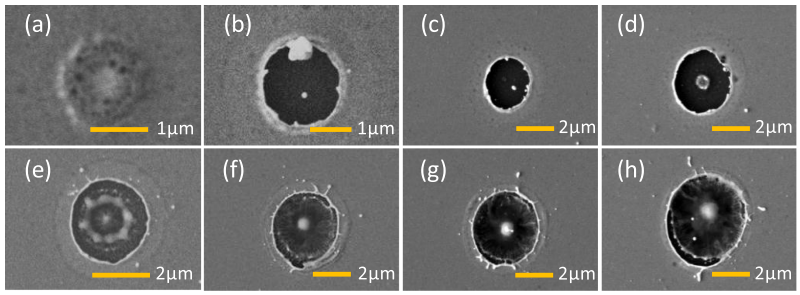

Fig. 5. (a)–(d) SEM images of the fabricated Au nanostructures at various pulse energies: (a) 2 nJ, (b) 4 nJ, (c) 6 nJ, and (d) 8 nJ. (e)–(h) SEM images of Si nanostructures based on the corresponding pre-processed Au nanostructures presented in (a)–(d).

the poor control of the fabricated nanostructures. In the following, we will discuss the fine control of the fabricated Si nanodome by weakening the polarization-dependent anisotropic effect.

The ultrashort period and ultrahigh intensity properties make fs laser–material interaction a nonlinear and nonequilibrium process, which limits the modified zone to the central area of the focal spot. Thus, a minor disturbance (energy fluctuation, surface defect etc.) causes a sizeable effect in the processing results. In our study, this effect is minimized through a confined electromagnetic field by controlling the SPPs scattering. Also, it can be controlled by the irradiated spot size. As presented in Figs. 5(a)–(d), Au nanostructures are fabricated through the $10\times$ objective (NA $= 0.25$) with a focal spot size of 4 μm. A sequential formation of thinner modification area (Fig. 5(a)), through hole with one bumped circle (Figs. 5(b) and 5(c)), and concentric surface structures with two bumped circles (Fig. 5(d)) is observed by increasing the pulse energy from 2 nJ to 8 nJ. Notably, concentric surface structure with three circles could not be found due to the small laser interaction area. Based on the Au nanostructures, a Si crown-like nanostructure (Fig. 5(e)) and nanodome (Figs. 5(f)–(h)) are fabricated due to the directed molten materials transport. Specially, the morphology of the Si nanodome with relatively small focus spot size is optimized with more symmetrical properties compared with that large focus spot size. Furthermore, the decrease in the entire interaction area facilitates the large-area nanodome with smaller adjacent spacing. Further simulation results show that the circularized incident laser induces a symmetric electric field concentration (Figs. 4(g)–(i)) compared with that in linear polarizations. In this condition, the molten Si are driven towards the central area by the surface tension in all radial directions, leading to the fine control of the resulted nanodome morphology. Thus, the polarization control combine with the tightly focusing condition enable the fine control of Si nanostructures (see Figs. S3 with the fabricated large-area nanodome structures under circular polarization).

4. Conclusion

This study proposed an effective method of manipulating Si nanostructures based on preprocessed planar Au nanostructures through modulating the electromagnetic field by controlling SPPs excitation and scattering. The abnormal annular-shaped fs laser pulse is used to imprint controllable planar nanostructures on Au thin films. Based on specific pre-processed Au nanostructures, bumped/sunken Si nanodomes/nanoholes can be fabricated by irradiating the nanostructures using a single shot dual-color fs laser pulse. Control of SPPs excitation and scattering by using pre-processed Au nanostructures is proposed as the primary mechanism for modulation of Si nanostructures. The underlying physical mechanism is verified by conducting a numerical simulation with the FDTD technique. The simulation results show that the specific lateral temperature profile can be induced by conducting directional SPPs manipulation through Au nanostructures, leading to surface tension driven transport of the molten Si to the center/periphery of the confined SPPs field. Thus, bumped Si nanodome and sunk nanohole can be fabricated upon solidification. Furthermore, the Si nanodome can be accurately fabricated as required by combining the focus

spot and polarization control. This study enables the formation of subwavelength nanostructures on bulk materials through modulation of the electromagnetic field by using quasi-plasmonic metallic nanostructures.

References

[1] Z. Deng *et al.*, "Fabrication of large-area concave microlens array on silicon by femtosecond laser micromachining," *Opt. Lett.*, vol. 40, pp. 1928–1931, 2015.
[2] P. A. Dmitriev *et al.*, "Laser fabrication of crystalline silicon nanoresonators from an amorphous film for low-loss all-dielectric nanophotonics," *Nanoscale*, vol. 8, pp. 5043–5048, 2016.
[3] Y. Gao *et al.*, "Photon-trapping microstructures enable high-speed high-efficiency silicon photodiodes," *Nature Photon.*, vol. 11, pp. 301–308, 2017.
[4] B. B. Xu, Y. L. Zhang, H. Xia, W. F. Dong, H. Ding, and H. B. Sun, "Fabrication and multifunction integration of microfluidic chips by femtosecond laser direct writing," *Lab Chip*, vol. 13, pp. 1677–1690, 2013.
[5] I. Paradisanos, C. Fotakis, S. H. Anastasiadis, and E. Stratakis, "Gradient induced liquid motion on laser structured black Si surfaces," *Appl. Phys. Lett.*, vol. 107, 2015, Art. no. 111603.
[6] M. L. Brongersma, Y. Cui, and S. Fan, "Light management for photovoltaics using high-index nanostructures," *Nature Mater.*, vol. 13, pp. 451–460, 2014.
[7] I. Rodriguez, L. Shi, X. Lu, B. A. Korgel, R. A. Alvarez-Puebla, and F. Meseguer, "Silicon nanoparticles as Raman scattering enhancers," *Nanoscale*, vol. 6, pp. 5666–5670, 2014.
[8] C. R. Szczepanski, F. Guittard, and T. Darmanin, "Recent advances in the study and design of parahydrophobic surfaces: From natural examples to synthetic approaches," *Adv. Colloid Interface Sci.*, vol. 241, pp. 37–61, 2017.
[9] F. Rigoni *et al.*, "A cross-functional nanostructured platform based on carbon nanotube-Si hybrid junctions: Where photon harvesting meets gas sensing," *Sci. Rep.*, vol. 7, 2017, Art. no. 44413.
[10] M. Naffouti *et al.*, "Templated solid-state dewetting of thin silicon films," *Small*, vol. 12, pp. 6115–6123, 2016.
[11] K. E. Chong *et al.*, "Observation of Fano resonances in all-dielectric nanoparticle oligomers," *Small*, vol. 10, pp. 1985–1990, 2014.
[12] E. G. Gamaly, *Femtosecond Laser-Matter Interaction: Theory, Experiments and Applications*. Boca Raton, FL, USA: CRC Press, 2011.
[13] L. Jiang, A. D. Wang, B. Li, T. H. Cui, and Y. F. Lu, "Electrons dynamics control by shaping femtosecond laser pulses in micro/nanofabrication: Modeling, method, measurement and application," *Light, Sci. Appl.*, vol. 7, 2018, Art. no. 17134.
[14] W. N. Han *et al.*, "Femtosecond laser induced concentric semi-circular periodic surface structures on silicon based on the quasi-plasmonic annular nanostructure," *Nanotechnol.*, vol. 29, 2018, Art. no. 305301.
[15] M. Shen *et al.*, "Formation of regular arrays of silicon microspikes by femtosecond laser irradiation through a mask," *Appl. Phys. Lett.*, vol. 82, pp. 1715–1717, 2003.
[16] U. Zywietz, C. Reinhardt, A. B. Evlyukhin, T. Birr, and B. N. Chichkov, "Generation and patterning of Si nanoparticles by femtosecond laser pulses," *Appl. Phys. A*, vol. 114, pp. 45–50, 2014.
[17] D. Zhang *et al.*, "A simple way to achieve pattern-dependent tunable adhesion in superhydrophobic surfaces by a femtosecond laser," *ACS Appl. Mater. Interfaces*, vol. 4, pp. 4905–4912, 2012.
[18] X. W. Li *et al.*, "Controllable Si (100) micro/nanostructures by chemical-etching-assisted femtosecond laser single-pulse irradiation," *Appl. Phys. Lett.*, vol. 110, 2017, Art. no. 181907.
[19] J. H. Yoo *et al.*, "Directed dewetting of amorphous silicon film by a donut-shaped laser pulse," *Nanotechnol.*, vol. 26, 2015, Art. no. 165303.
[20] C. Hnatovsky, V. G. Shvedov, N. Shostka, A. V. Rode, and W. Krolikowski, "Polarization-dependent ablation of silicon using tightly focused femtosecond laser vortex pulses," *Opt. Lett.*, vol. 37, pp. 226–228, 2012.
[21] J. P. Singer, P. T. Lin, S. E. Kooi, L. C. Kimerling, J. Michel, and E. L. Thomas, "Direct-Write thermocapillary dewetting of polymer thin films by a laser-induced thermal gradient," *Adv. Mater.*, vol. 25, pp. 6100–6105, 2013.
[22] M. G. Rahimian, F. Bouchard, H. Al-Khazraji, E. Karimi, P. B. Corkum, and V. R. Bhardwaj, "Polarization dependent nanostructuring of silicon with femtosecond vortex pulse," *APL Photon.*, vol. 2, 2017, Art. no. 086104.
[23] W. N. Han *et al.*, "Controllable plasmonic nanostructures induced by dual-wavelength femtosecond laser irradiation," *Sci. Rep.*, vol. 7, 2017, Art. no. 17333.
[24] J. Boken, P. Khurana, S. Thatai, D. Kumar, and S. Prasad, "Plasmonic nanoparticles and their analytical applications: A review," *Appl. Spectrosc. Rev.*, vol. 52, pp. 774–820, 2017.
[25] E. Ozbay, "Plasmonics: Merging photonics and electronics at nanoscale dimensions," *Science*, vol. 311, pp. 189–193, 2006.
[26] F. López-Tejeira *et al.*, "Efficient unidirectional nanoslit couplers for surface plasmons," *Nature Phys.*, vol. 3, pp. 324–328, 2007.
[27] Z. Fang *et al.*, "Plasmonic focusing in symmetry broken nanocorrals," *Nano Lett.*, vol. 11, pp. 893–897, 2010.
[28] A. G. Curto, G. Volpe, T. H. Taminiau, M. P. Kreuzer, R. Quidant, and N. F. van Hulst, "Unidirectional emission of a quantum dot coupled to a nanoantenna," *Science*, vol. 329, pp. 930–933, 2010.
[29] U. Zywietz, A. B. Evlyukhin, C. Reinhardt, and B. N. Chichkov, "Laser printing of silicon nanoparticles with resonant optical electric and magnetic responses," *Nature Commun.*, vol. 5, 2014, Art. no. 3402.
[30] P. B. Johnson and R. W. Christy, "Optical constants of the noble metals," *Phys. Rev. B*, 6, p. 4370, 1972.
[31] J. Bonse, A. Rosenfeld, and J. Krüger, "Implications of transient changes of optical and surface properties of solids during femtosecond laser pulse irradiation to the formation of laser-induced periodic surface structures," *Appl. Surf. Sci.*, vol. 257, pp. 5420–5423, 2011.